Applied Numerical Mathematics 7 (1991) 227–239
North-Holland

Review of incompressible fluid flow computations using the vorticity–velocity formulation

Thomas B. Gatski
Theoretical Flow Physics Branch, NASA Langley Research Center, Hampton, VA 23665-5225, USA

Abstract

Gatski, T.B., Review of incompressible fluid flow computations using the vorticity–velocity formulation, Applied Numerical Mathematics 7 (1991) 227–239.

An overview of the development of the vorticity–velocity formulation to the numerical solution of the Navier–Stokes equations is presented. The advantages and disadvantages to such a formulation are discussed, as well as the various numerical algorithms used in solving these governing differential equations.

1. Introduction

The traditional approach to the numerical solution of the incompressible Navier–Stokes equations has been to solve the "primitive variable" form of these equations. This constitutes solving the conservation of momentum equations, continuity equation (div $\boldsymbol{u} = 0$) and a pressure Poisson equation to obtain the $(\boldsymbol{u}, p)$ field. For planar or axisymmetric flow fields an equally popular approach has been to introduce a stream function, so the requirement of a solenoidal velocity field is automatically satisfied, and to reformulate the momentum equations into a vorticity transport equation by taking the curl of the velocity field. In three-dimensional flows, the extension of this approach is to introduce a vector-potential as well as the additional vorticity transport equation for the additional components of the vorticity (pseudo) vector.

There exists yet another, increasingly popular, approach to the numerical solution of the Navier–Stokes (N–S) equations. This is the numerical solution of the vorticity-velocity form of the N–S equations. This set constitutes the div $\boldsymbol{u} = 0$ and curl $\boldsymbol{u} = \omega$ equations (or an analogous derivable set), as well as the vorticity transport equation. The set is equally applicable in both two and three dimensions, although in three dimensions, the vorticity transport equation contains the additional term $\omega \cdot \nabla \boldsymbol{u}$, which acts as a vorticity production term. Before proceeding into the differential formulation of the vorticity–velocity equations and the development of the various numerical algorithms, it is helpful to examine some of the advantages and disadvantages of such a formulation.

Speziale [30] has shown that the vorticity–velocity formulation has the property that "non-inertial effects only enter into the solution of the problem through the implementation of initial and boundary conditions". In the primitive variable formulation, the mathematical character of

Elsevier Science Publishers B.V. (North-Holland)

the equations change. Therefore, whether doing problems in either inertial or, for example, rotating frames, the basic structure of the numerical algorithm does not have to be altered for the vorticity–velocity approach; whereas the changing character of the primitive variable equations may dictate the need for an alternate algorithm.

As is apparent from the formulation there is no pressure Poisson equation in the solution sequence. If the pressure field is required in the vorticity–velocity formulation, it is a consequence of the solution rather than an integral part of the solution procedure as it is in the primitive variable approach. This is an important consideration, since the issue of boundary conditions, in determining the pressure field, is still a matter of debate. (The reader is referred to two interesting and insightful papers on the subject by Orszag et al. [25] and Gresho and Sani [18].) On the other hand, the analogous question of vorticity boundary conditions is more straightforward in the vorticity–velocity approach. In the solution of the kinematic equations, that is the divergence and curl of the velocity field, either the normal or tangential component of the velocity field needs to be specified in order to get a unique solution. The imposition of the remaining velocity conditions through the curl equations then fixes the distribution of vorticity on the boundary. These points have been discussed by Wu [34] and Gatski et al. [17].

The vorticity–velocity approach, however, does require a solution for six dependent variables rather than the four dependent variables in the primitive variable approach for the full three-dimensional problem. In the two-dimensional case the number of unknown dependent variables reduces to three in both formulations. Thus, in the three-dimensional case, the vorticity–velocity approach does require more work (more equations need to be solved), although one obtains more information about the flow field in that two additional variables (additional vorticity components) associated with the flow field are obtained.

In Section 2 the differential formulation of the vorticity–velocity approach will be detailed, since the numerical algorithms have been developed for variations of the basic kinematic and transport equations. These numerical algorithms can be divided into three categories and these are discussed in Section 3 along with an historical development of the vorticity–velocity approach.

2. Formulation

For incompressible, unsteady flows of Newtonian fluids, the governing differential equations are:

$$\frac{\partial \boldsymbol{u}}{\partial t} + \boldsymbol{u} \cdot \nabla \boldsymbol{u} = -\frac{1}{\rho} \nabla p + \nu \nabla^2 \boldsymbol{u}, \tag{2.1}$$

$$\nabla \cdot \boldsymbol{u} = 0 \tag{2.2}$$

where $\boldsymbol{u}$ is the velocity vector, p is the pressure, ρ is the density and ν is the kinematic viscosity. The momentum equations can be re-expressed in terms of the vorticity by using the kinematic definition,

$$\nabla \times \boldsymbol{u} = \omega \tag{2.3}$$

and taking the curl of (2.1), that is,

$$\frac{\partial \omega}{\partial t} + \boldsymbol{u} \cdot \nabla \omega - \omega \cdot \nabla \boldsymbol{u} = \nu \nabla^2 \omega. \tag{2.4}$$

The pressure is now eliminated from the equations, although the resulting vorticity transport equation, (2.4), is, in some sense, more complex in that a new term, the "vortex stretching" term, appears in the equations. This term represents the process of generation (destruction) of vorticity due to the stretching (compression) of the vortex lines. In two dimensions, $\omega \cdot \nabla \boldsymbol{u}$ vanishes, and the vorticity transport equation reduces to a scalar equation for the component of vorticity normal to the planar motion of the fluid.

In order to establish a framework for the next section where the various numerical algorithms will be outlined and discussed, it is necessary to take the kinematic equation set, (2.2) and (2.3), one step further. The curl of (2.3) yields, using (2.2), the equation

$$\nabla^2 \boldsymbol{u} = -\nabla \times \omega. \tag{2.5}$$

Thus, an alternative to the solution of (2.2)–(2.4), is the set (2.4) and (2.5).

These equations are the basis for the differential formulation of the vorticity-velocity problem. However, in anticipation of the discussion of the next section, the solution of (2.2) and (2.3) can be written as (cf. [36])

$$\boldsymbol{u}(\boldsymbol{r}, t) = -\frac{1}{4\pi}\left[\int_V \frac{\omega_0 \times (\boldsymbol{r}_0 - \boldsymbol{r})}{|\boldsymbol{r}_0 - \boldsymbol{r}|^3}\, \mathrm{d}V_0 + \oint \frac{(\boldsymbol{u}_0 \cdot \boldsymbol{n})(\boldsymbol{r}_0 - \boldsymbol{r})}{|\boldsymbol{r}_0 - \boldsymbol{r}|^3}\, \mathrm{d}S_0 \right.$$
$$\left. - \int_S \frac{(\boldsymbol{u}_0 \times \boldsymbol{n}_0) \times (\boldsymbol{r}_0 - \boldsymbol{r})}{|\boldsymbol{r}_0 - \boldsymbol{r}|^3}\, \mathrm{d}S_0 \right] \tag{2.6}$$

where for this three-dimensional form, the integration is taken over a spherical surface with center at $\boldsymbol{r}_0$. This equation can take on many different forms depending on whether internal or external flow problems are considered and the applicable choice of boundary conditions. Equation (2.6), coupled with the vorticity transport equation, (2.5), represents the integro-differential vorticity–velocity formulation. This approach is somewhat outside the main thrust of the present paper; nevertheless, it is included here and discussed in the next section because of its historical relevance to development of the vorticity–velocity formulation. Note, that even though it bears some resemblance to the "vortex method", it is fundamentally different. In this integro-differential approach the vorticity is not represented by discrete point or line vortices and their images, rather it is a "continuous" function of the differential vorticity transport equation.

3. Algorithm development

The various numerical approaches to the solution of fluid flow problems using the vorticity–velocity formulation can be divided into three groups. These are:

(i) an integro-differential approach using a form of (2.6) and the vorticity transport equation, (2.4);
(ii) a differential approach using (2.2)–(2.4) (Method A); and
(iii) a differential approach using (2.5) and (2.4) (Method B).

In the following subsections, the contributions from various researchers to each of these methods will be discussed as well as a presentation of the different types of algorithms they have used or developed.

3.1 Integro-differential approach

As mentioned previously, this approach is somewhat outside the main thrust of this review, since it involves an integral formulation; however, its historical relevance to the numerical solution of flow problems using the vorticity–velocity approach dictates its inclusion. The work of Wu and his co-workers are highlighted here since they initiated this work in the early 1970s [35]. The basis of this development, as with all the vorticity–velocity formulations to be discussed, is the partition of the numerical procedure into a dynamic part and kinematic part. In all the approaches the dynamic part is represented by (2.4), whereas the kinematic part varies between methods.

Since (2.4) is parabolic, the evolution (temporal) of the vorticity field can be calculated once the initial vorticity distribution throughout the domain is known, and vorticity boundary conditions are specified on the boundary surface. An examination of (2.6) suggests that both the normal and tangential components of $\boldsymbol{u}$ can be specified [36]; however, this is subject to the integral constraints derivable from (2.2) and (2.3). Note that in this formulation as well as in the subsequent formulations to be discussed, the requisite vorticity boundary conditions are obtainable through (2.3); that is, the generation (destruction) of vorticity at the boundaries is a consequence of the kinematics of the problem. Wu [34] has analyzed the specification of boundary conditions associated with such an integral formulation as well as with the differential vorticity–velocity formulation.

This approach has been applied to a variety of time-dependent two-dimensional aerodynamic flow problems (e.g., [31]). Even though no formal analysis of the errors associated with the overall solution formulation has been performed, the numerical results, when compared to experimental results and other computational results, have been very favorable. By construction, the overall computational time associated with such a method is reduced, since it is not necessary to compute the entire flow field using (2.4). For wall-bounded flows, for example, the vorticity is confined to a relatively small portion of the domain; therefore, it is only necessary to solve the vorticity transport equation in the boundary-layer region. The integral formulation, (2.6), then allows for the velocity field to be computed, throughout the domain, from the "known" vorticity distribution.

3.2. Differential approach: Method A

This approach is the differential counterpart to the integro-differential method described in Section 3.1. It utilizes the continuity and curl equations, (2.2) and (2.3), as the kinematic equations to be solved, and (2.4) as the dynamic transport equation.

Gatski, Grosch and Rose (GGR [16,17]) have developed both a two-dimensional and a three-dimensional algorithm for the solution of the set (2.2)–(2.4). GGR [16] focused solely on the two-dimensional form of these equations, where the vorticity transport equation reduces to a single advective-diffusive *scalar* transport equation. GGR [17] extended the earlier two-dimensional version to three dimensions and further formalized the theoretical development of the algorithm. In both developments, the discretization scheme is compact; that is, it is a domain decomposition method in which the relationship between data and solution values in each element are expressed by algebraic relations and are extended throughout the domain by continuity requirements. To date, these have been formulated for Cartesian systems so that the resulting discretized equations are reminescent of the more familiar finite-difference forms.

The discrete approximations to the continuity and curl equations, (2.2) and (2.3), are derivable from Gauss' theorem and Stokes' theorem, respectively. The discrete scheme for the continuity equation is applicable over each volume element and the discrete scheme for the curl equations are applicable on the respective faces of each element. Thus, the velocity vector $\boldsymbol{u}$ is defined on the edges of each element. In GGR [17] box-variables were introduced and are defined at the vertices of each element.

The derivation of the discrete approximation scheme for the vorticity transport equation, (2.4), is more complex than that for the kinematic equations. First, it is assumed that the volume elements are sufficiently small so that the nonlinear differential operator in (2.4) can be approximated by an operator with constant (velocity, velocity gradient) coefficients. An "integrating factor" is then introduced, given by

$$\omega = \exp\left[\nabla \boldsymbol{u}^l (t - t_m)\right] \zeta \tag{3.1}$$

which reduces the "linearized" vorticity transport equation to the form

$$\zeta_t + (\boldsymbol{u}^l \cdot \nabla)\zeta = \nu \nabla^2 \zeta. \tag{3.2}$$

The coefficient $\boldsymbol{u}^l$ (and $\nabla \boldsymbol{u}^l$ as well) is now the "constant" velocity on an element at some iteration level l and time interval centered at $t = t_{\mathrm{m}}$. Note that the transport equations for the components of the vector ζ are no longer coupled through the vortex stretching term; rather, they are coupled through the matrix relation, (3.1), to the components of the vorticity vector ω. In the two-dimensional case, the transport equation for the vector ζ reduces to the scalar transport equation for the vorticity ω. The discrete approximation scheme to (3.2) is then obtained by applying Green's Theorem and obtaining polynomial solutions to the resulting adjoint equation (see [17] for details).

In the three-dimensional formulation, it is necessary that the vorticity be divergence free. This, of course, is a consequence of the kinematic differential relation, curl $\boldsymbol{u} = \omega$. In the GGR formulation, this is not explicitly enforced in the kinematic or dynamic part of the formulation. It is thus necessary that this compatibility condition on the discrete "vorticity" field be satisfied. This is accomplished by a Helmholtz decomposition of the computed field ω into a solenoidal and irrotational part. (Note that if $\nabla \cdot \omega \neq 0$ then the vector ω is *not* the vorticity.) The divergence operator applied to this decomposition yields the Poisson equation,

$$\nabla^2 \phi = \nabla \cdot \omega \tag{3.3}$$

where the right-hand side may be nonzero if the computed vector ω is not solenoidal. The solution of (3.3) (the irrotational vector $\nabla \phi$) can be used to project the computed vector field ω onto the space of divergence free ω ($\equiv \omega_{\mathrm{df}}$, the vorticity) by

$$\omega_{\mathrm{df}} = \omega - \nabla \phi. \tag{3.4}$$

Then the vorticity, ω_{df}, used in the kinematic part of the algorithm is compatible with the curl $\boldsymbol{u}$ operator.

The resulting set of linear algebraic equations from the discrete approximation schemes for both the kinematic and dynamic equations are solved using a method developed by Kaczmarz [17]. The method is analogous to an SOR method and with similar convergence rates. Since the solution method is independent of the ordering of the equations, the discrete schemes may be solved, element-by-element, either singly or in groups. In the case of the vorticity transport equation, it is also possible to construct an ADI algorithm for the solution of the discrete transport equation [16]. This is easily accomplished by equating fluxes at interfaces of adjacent elements. Tests have not been conducted on the algorithm to determine which is the most efficient for the solution of the vorticity transport equation.

The accuracy of both the two-dimensional and three-dimensional algorithms have been studied extensively ([16,17] respectively). For the three-dimensional case, two test problems were solved to check both the second-order spatial and temporal accuracy of the algorithm. For the spatial accuracy test, three-dimensional viscous stagnation point flow was studied, and for the temporal accuracy test, the problem of vortex spin-up was studied [17]. Both these tests have confirmed the second order spatial and temporal accuracy of the algorithm given second-order accurate boundary conditions. Tests were also run using first-order accurate boundary conditions on the vorticity. It was found, that away from the boundaries, the vorticity field remained second-order accurate while near the boundaries, the results deteriorated to first order for the vorticity. Nevertheless, the velocity field always maintained its second-order accuracy. Such problems of deteriorated accuracy near solid, boundaries, for example, are not uncommon. There, one-sided difference operators are sometimes employed to get the boundary vorticity; however, the loss in accuracy associated with the discretizations in these elements is then of the same order as the higher order accuracy associated with the discretizations in the larger-sized elements away from such boundary surfaces.

Both the two-dimensional and three-dimensional versions of the algorithms have been applied to flow problems other than the test cases mentioned previously. The two-dimensional version of the algorithm has been used in the study of surface drag effects over embedded cavities [14,15], and in the analysis of vortex coalescence in forced laminar mixing layers [23]. Some vortex pairing results from the forced mixing layer study are shown in Fig. 1. An essential feature of such transient dynamics is the ability to capture the streamwise spatial evolution of the vortices. Allowance for the spatial growth of the mixing layer, and the subsequent transverse shifting of the vortices, was essential to capturing the correct forced response behavior. Figure 1 shows the effect of phase angle on the response of the forced mixing layer. In addition to the forcing frequency, itself, the figure shows the retardation effect on mixing layer growth by varying the phase angle between the fundamental response frequency and the forcing subharmonic.

The three-dimensional algorithm has recently been used to study the phenomenon of vortex breakdown [28]. Figure 2 shows planar projected velocity vectors along the center-plane of a vortex breakdown bubble. The sequence of plots shows the temporal evolution of the internal bubble structure, particularly the injection/ejection of fluid in the aft portion of the bubble. Note that throughout this sequence, the overall bubble structure, which is rotating about the centerline, is fixed at a particular streamwise station by imposed free-stream pressure gradients.

The differential formulation of Method A has also been utilized by Osswald, Ghia and Ghia [26–28]; however, their approximation scheme and solution method differ from that of Gatski, Grosch, and Rose. They have developed their methodology for generalized orthogonal curvilinear coordinates. Direct matrix inversion techniques are used to solve the discrete approximation schemes to the kinematic equations, and an ADI-type method is used to solve the discrete approximation schemes to the vorticity transport equations.

The velocity and vorticity variables are staggered in each computational element; with the

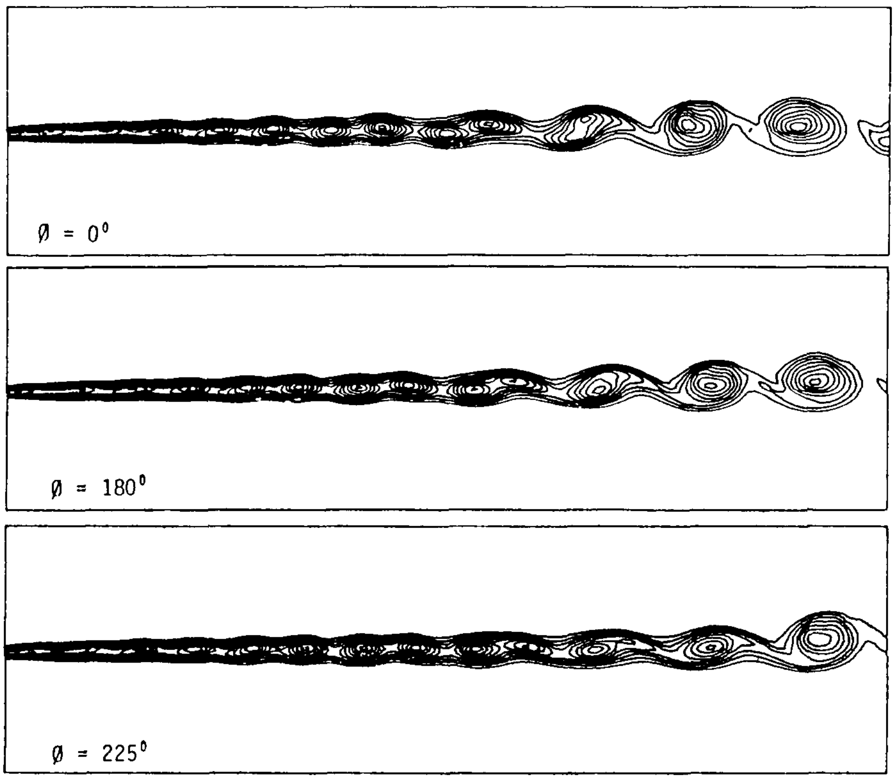

Fig. 1. Effect of phase angle on mixing layer evolution [23].

velocity components defined at the center of the respective coordinate surface, and the vorticity components defined at the mid-point of edges tangent to the respective component coordinate direction. The discretized divergence-curl equations are solved in conjunction with both compatibility and sufficiency conditions explicitly imposed on the system. This leads to a well-determined system in which the resulting solution matrix has a repetitive sparse block structure. This solution method is in contrast to the approach taken by Gatski, Grosch, and Rose; although the discrete analogs to both the compatibility constraint,

$$\nabla \cdot \omega = 0 \tag{3.5}$$

and the sufficiency conditions,

$$\int_S \boldsymbol{u} \cdot \boldsymbol{n} \; \mathrm{d}S = 0, \tag{3.6}$$

are also enforced in the GGR approach. In the GGR approach, boundary conditions are imposed such that (3.6) is enforced and (3.5) is satisfied by the Helmholtz projection described earlier in this subsection. Osswald, Ghia, and Ghia [26] extensively discuss the efficient direct solution of the divergence-curl equations as well as the stability and accuracy of the algorithm. They verified the second-order spatial accuracy of their divergence-curl algorithm by comparison with the analytical steady-state solutions of three-dimensional inviscid stagnation point flow and flow emanating from a point source. In both cases, the distribution of ω through the field was 0.

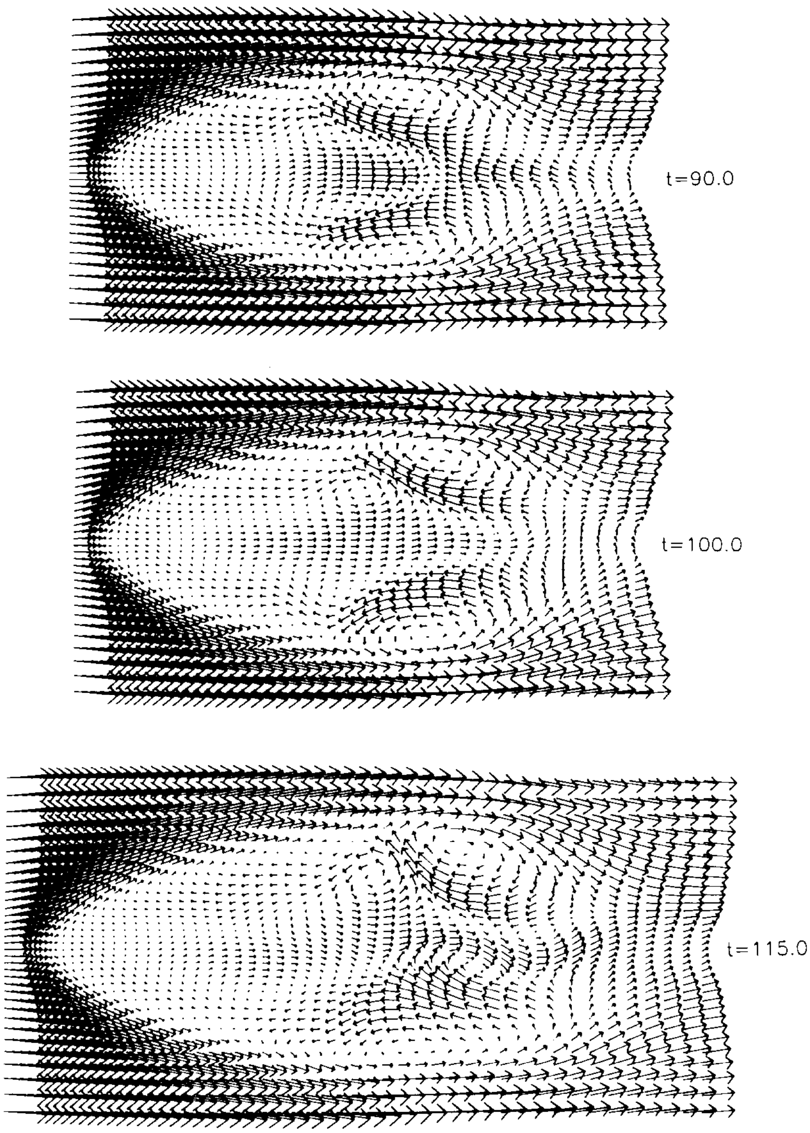

Fig. 2. Planar projected velocity vectors over the interior of the breakdown region at different time levels [29].

The analysis and validation of the algorithm for the vorticity transport equation was pursued separately. For the transport equation, a central spatial difference operator on both the diffusion and advection terms was used, and an implicit forward difference operator was used for the time derivative. The resulting discretization is formally second-order accurate.

Osswald, Ghia, and Ghia [26] have applied the full vorticity–velocity algorithm to the solution of the viscous flow within a shear driven cubical box. They studied the transient motion of the flow at Reynolds numbers of 100, based on box height and velocity of the top moving surface, and have continued the calculation onto steady state. Although no comparisons are made with other computations, the results presented appear consistent with other flow solutions within a box.

3.3. Differential approach: Method B

This approach involves the numerical solution of (2.4) and (2.5). It is the most widely used differential approach to the solution of the vorticity–velocity formulation. Fasel [7] appears to have been the first to employ such a formulation. Initially, this work was focused on the stability of boundary layers to small periodic perturbations and the study of the development of Tollmien–Schlichting waves [8]. The numerical method was fully implicit and was second-order accurate in both space and time. The solution of the difference equations used a line iteration method on the simultaneous iteration of the discrete equations. An additional feature was that on grid lines parallel to the y-direction (normal to the boundary surface), a direct method (e.g., Thomas algorithm) was used, while along the x-axis (streamwise) the solution proceeded iteratively. Later studies [11,10] focused on larger amplitude upstream perturbations and the subsequent nonlinear development of the two-dimensional disturbances in both boundary layer and Poiseuille flows. In addition, numerical studies were performed on a boundary-layer flow with a backward-facing step and subjected to an upstream perturbation [11]. These stability studies have been extended to fourth order accuracy and have also included the nonlinear growth of wave packets in boundary layers [9] and Poiseuille flow [2,3]. Temperature effects have also been incorporated into some of these studies (e.g. [1]). In addition, numerical studies have been made of the interaction between Tollmien–Schlichting waves and a laminar separation bubble [19], and the natural unsteadiness of boundary-layer flows over backward-facing steps [4]. The work has now been extended to the three-dimensional development of disturbances in a spatially growing boundary layer [12,13], using a variation of (2.5) for solution of the velocity field [20]. The spatial accuracy in these calculations is fourth-order and the spanwise coordinate is handled spectrally by Fourier decomposing in this direction. More accurate perturbation solution fields were obtained by first solving for the steady flow field, and then, by decomposing the solution field into the sum of the steady and unsteady (perturbation) fields, solving for the perturbation field, $\boldsymbol{u}'$ and ω'. Figure 3 shows instantaneous lines of constant vorticity in the x–y plane at the later stages of transition [13]. The figure shows the break-up of the instantaneous high shear layer into the smaller hairpin eddies. Further downstream, the motion is no longer periodic but rather random in nature. It may be important to recall at this point that in the vorticity–velocity

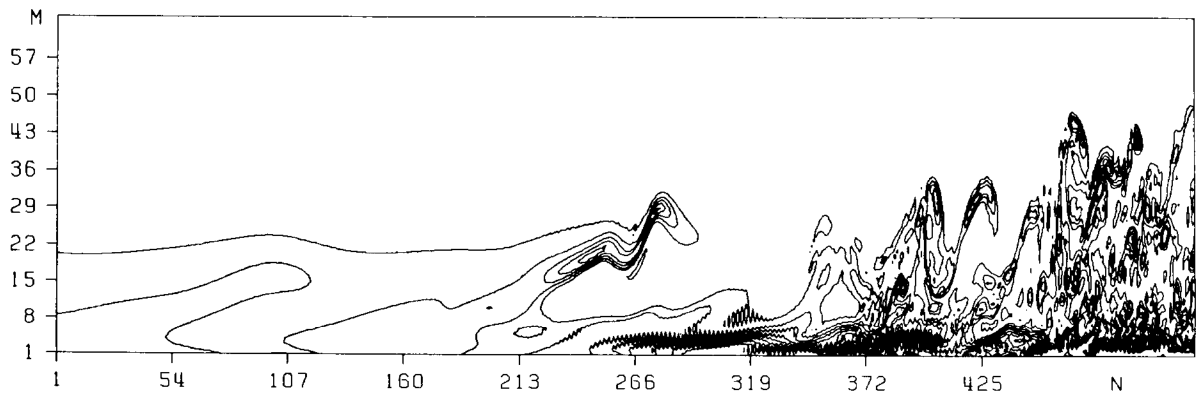

Fig. 3. Lines of constant vorticity (instantaneous) at later stages of transition [13].

formulation, the vorticity is a directly computable quantity and the accuracy of the vorticity is consistent with the accuracy of the algorithm; whereas in other formulations, where the vorticity is a derivable quantity, accuarcy is lost in taking derivatives of the discrete velocity field. In flows such as the ones displayed in the figures, where strong regions of shear dominate, poor accuracy in the vorticity field can lead to highly spurious results.

Many others have also utilized this approach; however, even though the governing differential equations are the same, that is (2.4) and (2.5), the discretization and solution of the resulting algebraic equations tend to differ. Dennis et al. [5] solved for the steady flow inside a cubical box for Reynolds numbers up to 100. Calculations at higher Reynolds numbers were possible but the accuracy of the solution could not be guaranteed. A second-order accurate central difference approximation was used for both the velocity Poisson equations and the steady vorticity transport equations. The resulting scheme for the velocity Poisson equations was diagonally dominant so that an over-relaxation parameter could be used in an iterative solution. Unfortunately, this was not the case for the vorticity transport equation, and it was necessary to apply a transformation which assumes a locally exponential solution to the linearized (local) vorticity transport equations. Central differences were used to obtain a set of algebraic equations representing the vorticity transport equations. Due to the exponential transformation, the matrix operator was not necessarily diagonally dominant. However, by expanding these exponentials about the local solution point and retaining terms of $O(h^2)$, it was possible to obtain matrix operators which were diagonally dominant. Iterative relaxation solution methods were then used, although the accuracy of the results were dependent on the size of the local cell Reynolds number.

Farouk and Fusegi [6] have applied the two-dimensional form of (2.4) and (2.6), coupled with an appropriate energy equation, to convective heat transfer problems in both a square cavity and horizontal circular annulus. Emphasis was placed on the solution of these test problems rather than the development of a new numerical algorithm, although an iteration procedure was introduced which solved for the vorticity and velocity simultaneously along a given coordinate line. The governing equations were discretized using a control volume based implicit finite-difference method. The coupled system of algebraic equations was solved using a block tridiagonal matrix algorithm. No formal accuracy checks were made on the resulting algorithm; however, second-order accurate finite-difference expressions were used for the vorticity boundary conditions implying the method is assumed second-order accurate. Free and forced convection problems were studied for the square cavity; and free and mixed convection problems were studied for the cylindrical annulus.

Cognizant of the previous developments in formulating the Navier–Stokes equations in terms of the vorticity and velocity, Orlandi [24] focused on developing a new, more efficient, numerical algorithm for the solution of the vorticity–velocity equations in two dimensions. He used an implicit time-splitting scheme in which the time and space discretization gives a linear system of algebraic equations. One of the intents was to eliminate any type of iterative procedure because of the increased CPU times, usually required of such algorithms, as the Reynolds number is increased. A staggered mesh was used so that the resulting discretization insured “exact” mass conservation as well as a block tridiagonal structure to the linear system of algebraic equations. An extensive analysis of the discretization of the nonlinear advection terms was performed to insure the second-order accuracy of the method and to more efficiently structure the resulting block tridiagonal matrices.

Two test cases were run to examine the stability and accuracy of the method; they were the driven cavity problem and the flow over a backward-facing step. For the driven cavity problem, steady-state results were obtained for a Reynolds number of 400. Tests were conducted to investigate the stability of the method, and it was found that for a coarse grid and cell Reynolds numbers greater than 2, no spatial oscillations occurred. Calculations for Reynolds numbers up to 6400 were also performed using stretched grids within the computational domain.

The results for the backward-facing step problem were less conclusive. In comparison with experiments, it appeared that numerical viscosity errors were introduced when non-uniform grids were used. Some discrepancies were found in comparisons with both the location of the reattachment point of the main separation region, and the detachment and reattachment locations of the upper separation region. Nevertheless, considering the high Reynolds number cases examined, especially in the backward-facing step case, the results for both test cases were in generally good agreement with experiments.

Finally, Ta Phuoc and his colleagues have used the vorticity–velocity formulation to solve for the flow over a three-dimensional backward-facing step in a channel [33] and the two- and three-dimensional flow over a circular cylinder [21,22]. The discretization of the equations was based on central spatial difference operators and an ADI method was used for the solution of the resulting tridiagonal system of linear algebraic equations. For the three-dimensional backward-facing step problem, Reynolds numbers (based on step height) of 150 and 400 were examined. An analysis of the separation zones within the flow field and the associated longitudinal vortices were performed; although, the analysis was qualitative since no comparisons with experiments or other numerical studies were made.

Labidi and Ta Phuoc [21,22] applied a slightly different ADI algorithm to the solution of two- and three-dimensional flow over a circular cylinder. The numerical scheme used is second-order accurate in space and time for the vorticity transport equations and second-order accurate for the velocity Poisson equations. In some cases, however, a fourth-order discretization in the radial direction was used to better satisfy the divergence-free condition on the velocity. Unfortunately, even the fourth-order discretization was not able to maintain a divergence-free velocity field for moderate-to-high Reynolds numbers. Following Takemitsu [32], they introduced a scalar potential function; and, in a manner analogous to the projection of the vorticity field described earlier (cf. [17]), they obtained, through an iterative process, a divergence-free velocity field at the end of each time step. A comparison between the temporal evolution of the velocity divergence (both the mean square error and maximum error value), for the case of an impulsively started flow over a circular cylinder ($\mathrm{Re} = 10^3$), clearly showed the improvement obtained by the introduction of the potential function.

For the three-dimensional flow case, a cylinder of finite length and bounded by two circular plates was studied. In addition to the explicit enforcement of the divergence-free condition on the velocity field, Labidi and Ta Phuoc [22] also found it necessary to explicitly enforce the divergence-free condition on the vorticity field as well. They studied the impulsively started flow over a circular cylinder at a Reynolds number of 300 for two different cylinder length-to-diameter ratios ($L/D = 5{,}10$). Relatively good agreement was found between the radial velocity distribution on the symmetry axis behind the cylinder, for both L/D ratios, and the radial velocity distribution for the two-dimensional cylindrical flow.

4. Concluding remarks

The intent of this review has been to highlight some of the work which has been conducted using the vorticity–velocity formulation. As has been shown, within the framework of the vorticity–velocity formulation, there are different integro-differential and differential approaches that can be followed. The major focus of the present review has been on the differential approaches, although the integro-differential approach has been included for both historical reasons and the close links which can be formed with the differential approaches.

The review has shown that the vorticity–velocity formulation is a viable approach to the solution of both two- and three-dimensional incompressible fluid flow problems. The number of research groups actively pursuing this formulation suggests that it is an attractive alternative to the primitive variable, pressure–velocity formulation. Certainly, one could anticipate that there are flow geometries and/or physical constraints which would dictate a preference for one formulation over another. However, this would not be a measure of whether one method is better than another, rather, it would be a choice of an optimal formulation which best serves the efficiency and/or accuracy requirements of the flow problem at hand.

Clearly, with the research effort presently being exerted in the utilization of the vorticity–velocity formulation, more complex flow problems will be studied and more efficient algorithms will be developed for both two- and three-dimensional unsteady incompressible fluid flow problems.

References

[1] H. Bestek and H. Fasel, Numerische Simulation zweidimensionaler Wellenpakete in der ebenen Poiseuille-Stromung, *Z. Angew. Math. Mech.* 65 (1985) T182–T185.

[2] H. Bestek and H. Fasel, Numerical simulation of laminar-turbulent transition, in: *Proceedings 11th IMACS World Congress on System Simulation and Scientific Computation*, Oslo, Norway (1985).

[3] H. Bestek, P. Ditrich and H. Fasel, Einfluss der Wandtemperatur auf die Entwicklung von Tollmien-Schlichting-Wellen in Grenzschichlstromungen, *Z. Angew. Math. Mech.* 67 (1987) T256–T258.

[4] H. Bestek, K. Gruber and H. Fasel, Numerical investigation of unsteady laminar boundary layer flows over backward-facing steps, in: *Proceedings Fourth Asian Congress of Fluid Mechanics*, Hong Kong (1989).

[5] S.C.R. Dennis, D.B. Ingham and R.N. Cook, Finite-difference methods for calculating steady incompressible flows in three dimensions, *J. Comput. Phys.* 33 (1979) 325–339.

[6] B. Farouk and T. Fusegi, A coupled solution of the vorticity–velocity formulation of the incompressible Navier–Stokes equations, *Internat. J. Numer. Methods Fluids* 5 (1985) 1017–1034.

[7] H. Fasel, Numerische Integration der Navier–Stokes Gleichungen fur die zweidimensionale, inkompressible Stromung langs einer ebenen Platte, *Z. Angew. Math. Mech.* 53 (1973) T236–T238.

[8] H. Fasel, Investigation of the stability of boundary layers by a finite-difference model of the Navier–Stokes equations, *J. Fluid Mech.* 78 (1976) 355–383.

[9] H. Fasel, Numerical simulation of nonlinear growth of wave packets in a boundary layer, in: T. Tatsumi, ed., *Turbulence and Chaotic Phenomena in Fluids* (North-Holland, Amsterdam 1984) 31–37.

[10] H. Fasel and H. Bestek, Investigation of nonlinear, spatial disturbance amplification in plane Poiseuille flow, in: *Proceedings IUTAM-Symposium on Laminar-Turbulent Transition*, Universitat Stuttgart, Stuttgart, FRG (1979).

[11] H. Fasel, H. Bestek and R. Schefenacker, Numerical simulation studies of transition phenomena in incompressible, two-dimensional flows, in: *Proceedings AGARD Symposium on Laminar-Turbulent Transition*, Technical University of Denmark, Copenhagen, Denmark (1977).

[12] H. Fasel, U. Rist and U. Konzelmann, Numerical investigation of the three-dimensional development in boundary layer transition, in: *Proceedings AIAA 19th Fluid Dynamics, Plasma Dynamics and Laser Conference*, Honolulu, HI (1987); Paper No. 87–1203.

[13] H. Fasel, U. Rist and U. Konzelmann, Numerical simulation of later stages of transition in a growing boundary layer, in: *Proceedings Fourth Asian Congress of Fluid Mechanics*, Hong Kong (1989).
[14] T.B. Gatski, Drag characteristics of unsteady, perturbed boundary layer flows, in: *Proceedings AIAA Shear Flow Control Conference*, Boulder, CO (1985); Paper No. 85-0551.
[15] T.B. Gatski and C.E. Grosch, Embedded cavity drag in steady Laminar flow, *AIAA J.* 23 (1985) 1028–1037.
[16] T.B. Gatski, C.E. Grosch and M.E. Rose, A numerical study of the two-dimensional Navier–Stokes equations in vorticity–velocity variables, *J. Comput. Phys.* 48 (1982) 1–22.
[17] T.B. Gatski, C.E. Grosch and M.E. Rose, The numerical solution of the Navier–Stokes equations for three-dimensional unsteady, incompressible flows by compact schemes, *J. Comput. Phys.* 82 (1989) 298–329.
[18] P.M. Gresho and R.L. Sani, On pressure boundary conditions for the incompressible Navier–Stokes equations, *Internat. J. Numer. Methods Fluids* 7 (1987) 1111–1145.
[19] K. Gruber and H. Bestek, Interaction between a Tollmien–Schlichting wave and a laminar separation bubble, in: *Proceedings AIAA 19th fluid Dynamics, Plasma Dynamics and Laser Conference*, Honolulu, HI (1987); Paper No. 87-1256.
[20] U. Konzelmann, U. Rist and H. Fasel, Numerical investigation of the effects of longitudinal vortices on the onset of transition in a flat plate boundary layer, in: *Proceedings AGARD/FDP Symposium*, Cesme, Turkey (1988).
[21] W. Labidi and L. Ta Phuoc, Numerical resolution of the Navier–Stokes equations in velocity–vorticity formulation: Application to the circular cylinder, in: M. Deville, ed., *Proceedings 7th GAMM Conference on Numerical Methods in Fluid Dynamics* (Vieweg, Braunschweig, 1988).
[22] W. Labidi and L. Ta Phuoc, Numerical resolution of the three-dimensional Navier–Stokes equations in velocity–vorticity formulation, in: *Proceedings 11th International Conference on Numerical Methods in Fluid Dynamics*, Williamsburg, VA (1988).
[23] R.M. McInville, T.B. Gatski and H.A. Hassan, Analysis of large vortical structures in shear layers, *AIAA J.* 23 (1985) 1165–1171.
[24] P. Orlandi, Vorticity–velocity formulation for high Re flows, *Comput. & Fluids* 15 (1987) 137–149.
[25] S.A. Orszag, M. Israeli and M.D. Deville, Boundary conditions for incompressible flows, *J. Sci. Comput.* 1 (1986) 75–111.
[26] G.A. Osswald, K.N. Ghia and U. Ghia, A direct algorithm for solution of three-dimensional unsteady Navier–Stokes equations, in: *Proceedings AIAA 8th Computational Fluid Dynamics Conference*, Honolulu, HI (1987); Paper No. 87-1139.
[27] G.A. Osswald, K.N. Ghia and U. Ghia, Direct solution methodologies for the unsteady dynamics of an incompressible fluid, in: S.N. Atluri and G. Yagawa, eds., *Proceedings of the International Conference on Computational Engineering Science* 2 (Springer, New York, 1988).
[28] G.A. Osswald, K.N. Ghia and U. Ghia, Direct method for solution of three-dimensional unsteady, incompressible Navier–Stokes equations, in: *Proceedings 11th International Conference on Numerical Methods in Fluid Dynamics*, Williamsburg, VA (1988).
[29] R.E. Spall, T.B. Gatski and R.L. Ash, The structure and dynamics of bubble-type vortex breakdown, *Proc. Roy. Soc. London Ser. A* 429 (1990) 613–637.
[30] C.G. Speziale, On the advantages of the vorticity–velocity formulation of the equations of fluid dynamics, *J. Comput. Phys.* 73 (1987) 476–480.
[31] A. Sugavanan and J.C. Wu, Numerical study of separated turbulent flow over airfoils, *AIAA J.* 20 (1982) 464–470.
[32] N. Takemitsu, Finite difference method to solve incompressible fluid flow, *J. Comput. Phys.* 61 (1985) 499–518.
[33] A. Toumi and L. Ta Phuoc, Numerical study of three-dimensional viscous incompressible flow by vorticity and velocity formulation, in: *Proceedings 5th International Conference on Numerical Methods in Laminar and Turbulent Flow*, Montreal, Que (1987).
[34] J.C. Wu, Fundamental solutions and numerical methods for flow problems, *Internat. J. Numer. Methods Fluids* 4 (1984) 185–201.
[35] J.C. Wu and J.F. Thompson, Numerical solution of unsteady, three-dimensional Navier–Stokes equations, in: *Proceedings Project SQUID Workshop on Fluid Dynamics of Unsteady, Three-Dimensional, and Separated Flows*, Lafayette, IN (1971) 253–280.
[36] J.C. Wu and J.F. Thompson, Numerical solution of time-dependent incompressible Navier–Stokes equations using an integro-differential formulation, *Comput. & Fluids* 1 (1973) 197–215.